Assessment of the influence of sources of error on the total error budget of GBOT observations

prepared by: Martin Altmann, Sebastien Bouquillon, Francois Taris, Alexandre Andrei, Sebastian Els, Iain Steele, Richard Smart

approved by:
reference: GAIA-C3-TN-ARI-MA-009-01
issue: 01
revision: 0
date: 2012-11-15
status: Issued

Abstract

Given the high aims of GBOT in terms of precision and accuracy, an assessment of the influences of various effects on the GBOT observations is required. This is described in this document.

Contents

1 Introduction

The commitment of GBOT in terms of precision is 20 mas per daily sequence. The maximum allowed inaccuracy is even smaller, however at current not specified in numbers. With this ambitious goal in mind, all potential effects that might adversely affect the measurements need to be assessed in order to see whether they are indeed significant, and if this is the case, how large the magnitude of their influence is. Furthermore methods to eliminate or at least minimise the impact of these mostly systematic influences need to be considered.

The main effects can roughly be divided into these groups:

- **Physical effects:** These originate from the physical properties of light and its passage through moving transparent bodies, such as Earth's atmosphere. of matter. Physical effects include all varieties of refraction, aberration, gravitational light deflection, etc.
- **Astronomical and meteorologic effects:** These reflect the astronomical properties of our surroundings, i.e. the ambient conditions for a given set of observations. Examples are: Seeing, lunar phase and proximity, altitude, sky transparency, field density. Since most of these are transient, they will cause a systematic effect on a given observing sequence, but unlikely a large scale influence. Nonetheless, some of these are of high significance, especially in combination with other effects.
- **Optical effects:** Strictly speaking these are part of the first group, but since optics play such an overwhelming role in observational astrometry it is wise to put the optical effects into their own group, especially since the scope of their significance is somewhat different compared to that of the former effects. Moreover they are all localised in one part of the process, namely the telescope/instrument itself. This also means that a large part of their systematicality is limited to the individual telescope (or groups of telescopes) rather than being global.
- **Technical effects:** These are all of those items, which do not originate from the actual instrument. Examples for these are the accuracy of the timestamp, and the observatory coordinates. For these limits have been established before. While not related to the facility as such, all influences stemming from the reference catalogues, coordinate systems, etc. should also be included into this category.
- **Miscellaneous effects:** all other effects

Changes of the reference frame, e.g. induced by precession and nutation of the earth are not reflected in the measurements of GBOT. GBOT will deliver its astrometric data in the IGSL and in J2000 coordinates. The astrometry conducted by GBOT is small field astrometry hinged to a reference catalogue. All of the available reference catalogues are also in these coordinates. For the problems resulting from the finite accuracy of the reference catalogues on various scales, see Sect. 2.5.3.

It is to be noted, that, since GBOT will not be able to fully reach it's commitment before all observations were re-reduced using Gaia's own results as reference material, the magnitude and influence of some of the effects dealt with in this document will be hidden or even change. Therefore this report can at this time only be considered a preliminary report. It will be expanded and updated regularly in the future.

2 Effects contributing to the total error of GBOT observations

2.1 Physical effects

2.1.1 Aberration

The physical aberration is caused by movement of the measuring device (i.e. telescope/detector) perpendicular to its optical axis and the fact that the speed of light is finite. This means that light entering an optical setup needs a minute but non-negligible amount of time to travel through the optics, during which the (moving) apparatus has moved perpendicular to the motion of the light , which leads to a displacement of the ray in this direction. This effect is very large, indeed the effect of aberration is one of the two main reasons why GBOT was installed in the first place. However, in contrast to Gaia, which has two FOV's about 107°apart, thus always moving with two different velocities perpendicular to the infalling light rays as the space probe follows its scan law, our GBOT observations have one FOV, and the FOV is small. Therefore the vast bulk of the effect, which can amount to more than 20" in case of an earth bound observer is cancelled out, since the perpendicular motion is almost the same for all incident light. However, there is a small residuum due to differential aberration, which needs to be taken care of for full accuracy.

The treatment here in will be limited to the classical non-relativistic non-post Newtonian approach. Though the differences from the relativistic to the classical approach are below 1 milliarcsec, as far as they are treated as second-order effects of the latter, they might be of systematic nature given the repeated pattern of motion of the probe. In such a case it might be interesting to derive the quantities. This can only be envisaged for some time months ahead - for instance with the help of the relativity astrometry group in Turin.

The effects can be divided in Annual Aberration, Diurnal Aberration, and Light-time Correction

2.1.1.1 Annual Aberration Neither the L2 point nor the Gaia probe, on its Lissajous motion, completely follow the Earth's movement around the Sun. Indeed Gaia may venture up to 100,000km from the ecliptic, and at a speed commensurable with Earth's translation velocity. However the proximity of Gaia from Earth's and its rapid varying, complex movement about L2 render it much simpler to account for it as a light-time correction.

This accepted, no annual aberration as such befall to Gaia's apparent position. However, it of course does upon the stars positions relatively to which the probe's position will be determined. Correspondingly, a compensation term will have to be applied on Gaia position derived from stellar positions referred to the ICRS origin.

Since the largest value of the Sun-Gaia-Earth angle is about 5.3 degrees from the ecliptic, the differential aberrational corrections within the local stellar frame won't be larger than about 3 mas - and that only at Earth's peri- and aphelion, if these are combined with the maximal departure of the Lissajous-orbit from the Ecliptic. The correction for the differential aberration will be automatically done with the astrometric solution for the field.

2.1.1.2 Diurnal Aberration The situation here is opposite from the previous item, as Gaia's probe will share the same displacement as the stellar field. For typical observing scenarios, i.e. a 5-10' field, observations relatively close to the meridian, the differential corrections will be small, i.e. in the order of 1 mas, which again means, that they will be taken care of sufficiently in the course of the astrometric reduction.

2.1.1.3 Light time correction This effect is also caused by the fact that the velocity of light is finite, and that the true position of Gaia at the time of measurement will be off by the distance the spacecraft travels during the time that light requires from Gaia to the observer. The order of magnitude of this effect is 5 km (0.7 mas) for a relative spacecraft velocity of 1 km/s at the typical distance of 1.5 million km. Since GBOT does not have access to the precise distance to Gaia, this correction needs to be done by ESOC.

2.1.2 Refraction

Earth's atmosphere acts as a lens, i.e. incoming light gets refracted, i.e. displaced from it's original trajectory/direction. Moreover as it is the case with all lenses, the air in the atmosphere also holds the properties of a weak prism, i.e. refracting and thus splitting up light of different wavelengths in different ways. Since this effect can be rather large, it needs to be analysed and taken into account. Fortunately, as we'll see the bulk of the effect gets cancelled out in small field astrometry.

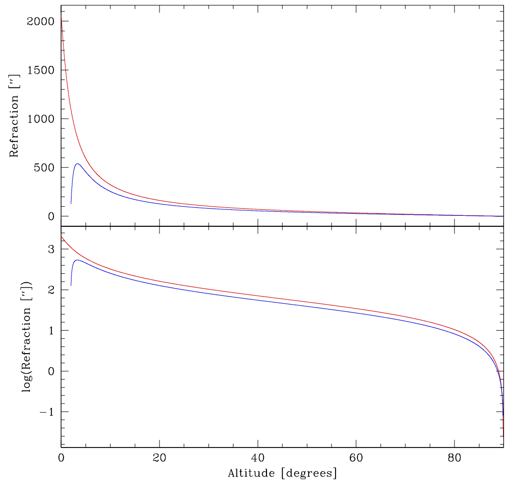

FIGURE 1: left: Sunset photograph showing the effects of differential refraction (the absolute part can only be perceived, if one compares the theoretical time of sunset with the observed one). Due to a very strong DR at the horizon, the Sun is very much flattened. Inhomogeneous layers of air additionally deform the solar image (Photo taken in Jan. 2009 at La Silla, Chile by MA with a Nikon D90). Right: Refraction function (Eqn. 5) as developed by Bennett (1982) in comparison with the well known LaPlace formula (Eqn. 4). Please note that the ambient conditions (air pressure, temperature) are a bit different for each of the curves. This way a distinction of the two curves, and a comparison is easier.

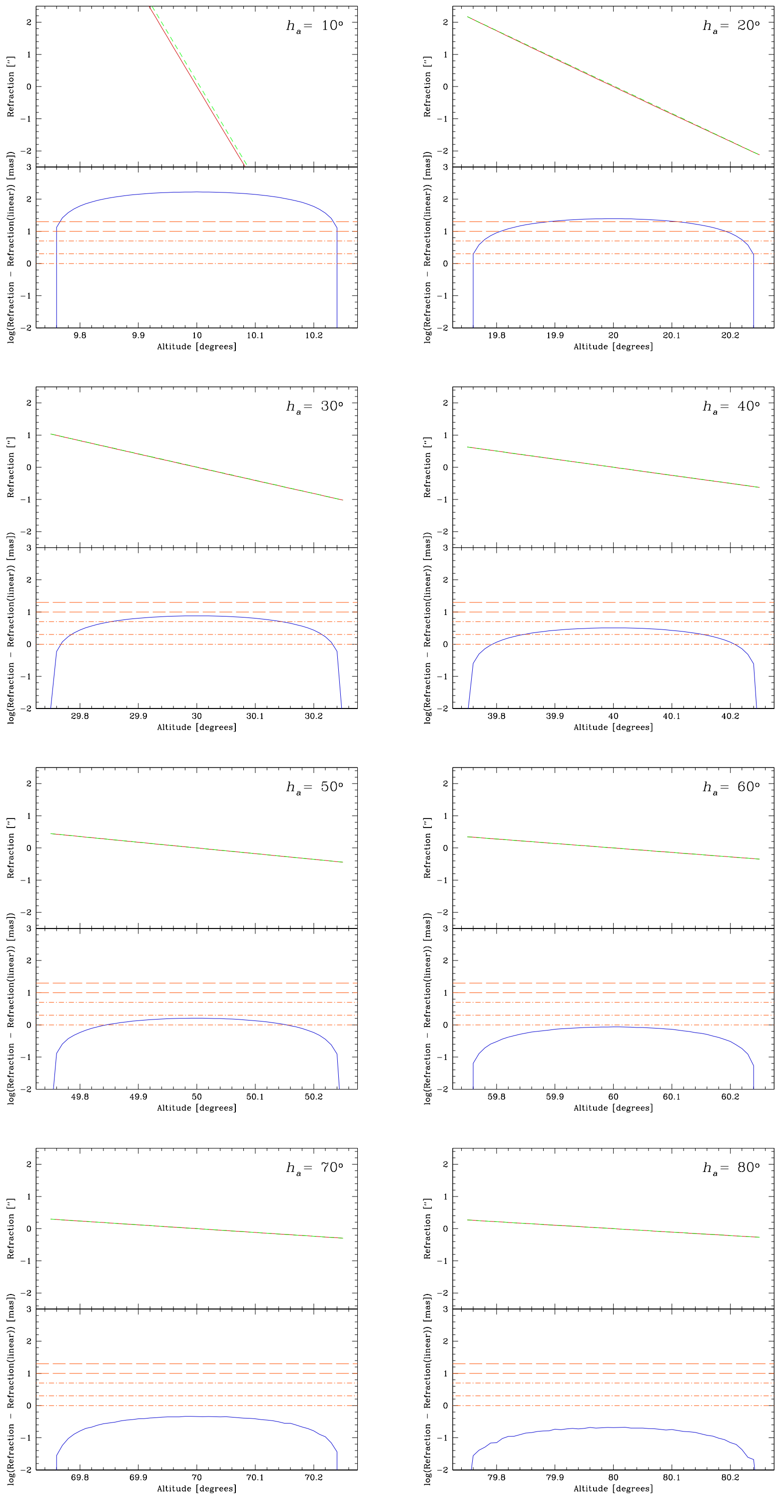

FIGURE 2: Differential refraction in fields of 30' centred on altitudes from 10°to 80°above horizon in steps of 10°. For each panel the upper plot shows the DR function (red solid line) and a linear equation fixed on the most extreme points of the field (green dashed line), while the lower plot shows the logarithm of the difference of the two. The orange long dashed lines denote the maximum errors, GBOT has committed itself to (using Gaia data) of 10 and 20 mas, the dot-dashed lines show the 1,2,5 mas limits for orientation purposes. Note how the slope of the DR function decreases significantly with higher altitudes, see also Tab. 2.1.2.2.

2.1.2.1 Absolute Refraction With absolute refraction we mean the total displacement of a ray of light transversing the atmosphere at a given zenithal distance. This is a very large effect, especially near the horizon, where it can amount to more than 30' (1800"), which means, that if one watches the Sun rise of set, it actually already has set (or not yet risen), one only sees the Sun's[1] image. Fortunately the magnitude of this effect quickly diminishes, so that is much more reasonable in the parts of the sky where observations usually take place. With the absolute refraction being defined as

$$R = z - z_0 \tag{1}$$

with z_0 being the observed zenithal distance (from ground level), and z the actual one (i.e. without an atmosphere), the refraction can be expressed as the following integral for a radially symmetric atmosphere, given by Green (1985):

$$R = r_0 n_0 \sin z_0 \int_1^{n_0} \frac{\mathrm{d}n}{\sqrt{n(r^2n^2 - {r_0}^2{n_0}^2 \sin {z_0}^2 z_0}} \tag{2}$$

with: n being the refractive index at distance r from the centre of the Earth, n_0 the refractive index at ground level, and r_0 the distance of observer to Earth's centre,

which can then be transformed to

$$R = -\int_0^{z_0} \frac{r\mathrm{d}n/\mathrm{d}r}{n + r\mathrm{d}n/\mathrm{d}r} \mathrm{d}z \tag{3}$$

Because the atmosphere is not homogeneous, but consists of layers, especially in the lowest part, the exact calculation of atmospheric refraction is complicated. However approximate models exist, such as the one by Sinclair & Hohenkerk (1985), which makes assumptions concerning the temperature and pressure gradients in our atmosphere, etc., see Gubler & Tytler (1998) for the full set of constraints. The integral given in equation 3 can then be expanded to obtain the Laplace expression:

$$R(\lambda) = A(\lambda) \tan z_0 + B(\lambda) \tan^3 z_0 \tag{4}$$

with $A(\lambda)$ and $B(\lambda)$ being functions depending on λ the temperature and the air pressure (seeGubler & Tytler (1998)). For $\lambda = 650$ nm, T=278 K, a pressure of 800 mb, $A = 46.57012$ and $B = -0.0514593$. This expression is good to more or less zenithal distances of 70°(see Fig. 1). Bennett (1982) has developed a formula, based on the politropic approach of Garfinkel (1967), who developed an algorithm based on the US Standard Atmosphere:

$$R = cot(h_a + \frac{7.31}{h_a + 4.4}) \tag{5}$$

[1] or any other light source from outside the atmosphere

which is valid for apparent altitudes. A plot for this relation is shown in Fig. 1. For the true altitude the following approximation is valid (Saemundsson, 1986), agreeing with the previous formula to 10':

$$R = 1.02cot(h + \frac{10.3}{h + 5.11}) \quad (6)$$

Since the optical properties of gases such as those in our Earth's atmosphere are dependent on both pressure and temperature, the equations cited above need to be corrected for this to become (Meeus, 1992):

$$R = cot(h_a + \frac{7.31}{h_a + 4.4}) \times \frac{P}{1010}\frac{283}{273 + T} \quad (7)$$

and

$$R = 1.02cot(h + \frac{10.3}{h + 5.11}) \times \frac{P}{1010}\frac{283}{273 + T} \quad (8)$$

To conclude it should again be noted, that all of these models are approximations only, the true atmosphere is much more structured and complicated.

Despite it's large size, absolute refraction plays no role in our context, since it affects all stars at a given zenithal distance in the same way. However minor effects persist, as described in the next two items.

2.1.2.2 Differential Refraction As said previously, the large effect of "absolute refraction" does not affect small field astrometry. However this is not exactly true, since even a small field will cover a range of zenithal distances, therefore a residual differential refraction (DR) effect remains. Of course, the larger the field, the larger this differential signal. Again, the DR is largest at low altitudes. In fields with ample numbers of stars the effect will be accommodated for in the fit. However, this means the addition of more free parameters, which may present problems in sparse fields. One approach to correct for DR without explicitly adding it as free parameters to the fit would be to correct by a linear approximation in the h direction. This would be acceptable to zenithal distances of about 40°(i.e. h_a=50°), see Tab. 2.1.2.2 (3rd column). However it may be more prudent to use a more exact formula, such as the ones given above.

In reality, the astrometric reduction consists of a n-order polynomial fit of the $\alpha\delta$-coordinates of a reference catalogue to the measured x, y-positions of the sources on the image frame. This means that to certain extent, the DR will already be corrected for. In many cases, however, the order of the polynomial will be limited to first order, meaning that also the DR will only be corrected to 1st order. Therefore the discussion concerning the difference between linear and true correction of the DR is not only an academic one, but for optimal results correcting this residual difference may be indicated.

In any case differential refraction needs to be taken care of (see Tab. 2.1.2.2, 2nd column), even at high altitudes. The values in Tab. 2.1.2.2 are computed for a field of 30' which is about

TABLE 1: Magnitudes of differential refraction over an 30' field centred on h_a(central)

h_a(central) [°]	DR [$''$]	$DR - DR_{\text{lin}}$ mas
10	15.19	167.60
20	4.29	24.74
30	2.06	7.61
40	1.25	3.21
50	0.88	1.61
60	0.70	0.87
70	0.59	0.46
80	0.54	0.21
90	0.52	0.01

the largest field to be used by GBOT. Moreover, one should abstain to observe at altitudes of less than 30°, the altitude at which the refraction, and with it the differential refraction starts to explode. This holds even more true, since light coming from sources lower than this in the sky spends more time in the lower disturbed layers of the atmosphere, which makes non-monotonous DR, which is hard to correct for, much more apparent and thus significant.

2.1.2.3 (Differential) Colour Refraction Differential refraction, as described in the previous paragraph is not the only residual effect arising from atmospheric refraction. Of similar magnitude, and a bit more complicated and more difficult to compensate is differential colour refraction (DCR). The origin of this is that light of different frequency is refracted by different amounts. Most astronomical objects have continuum SEDs therefore the atmosphere smears out their point spread functions to little spectra[2]. Since astronomical observations in general involve filters of some sort, these "spectra" are truncated. With filters the DCR effect is less severe. Would all stars have the same SED the DCR would show up as a general displacement, but the SEDs of stars differ widely. This then results in a colour dependent differential refraction effect, the DCR. Thus the loci of predominantly blue stars would be displaces in respect to those having mostly red light. The broader the passband of the filter the more pronounced this effect is. Line filters do not suffer from any significant DCR, since they only transmit a very small amount of the optical spectrum. However this means that they also transmit very little light overall, making them less suitable for astrometry of faint objects.

This means that we will have to assess the gravity of and correct for DCR. Refraction is less the redder one goes. In the NIR it is almost negligible. In I band[3] the DCR is still very small, in R

[2]since the total displacement is far less than the usual FWHM of the PSF, the dispersion manifests itself visually only in a slightly elongated image, if at all.

[3]for ease of the argument, the Johnson-Cousins designations are given here, in principle this also refers to

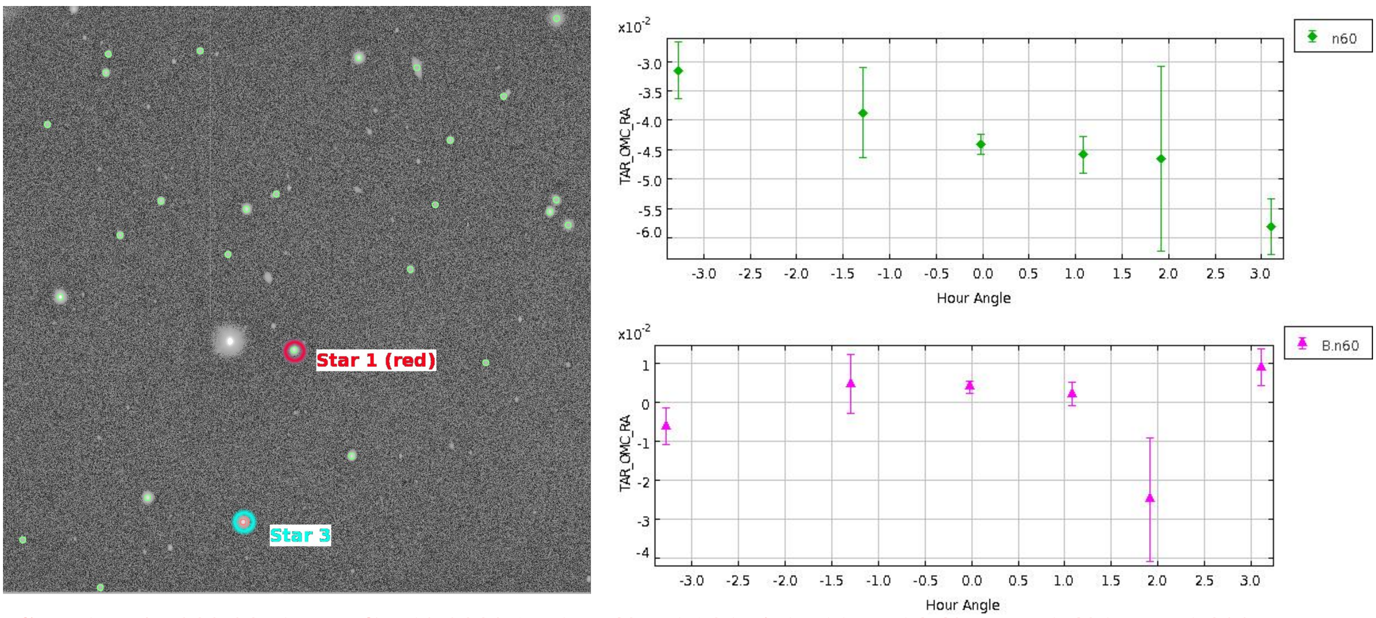

Star 1: RA: 239.98515 DEC:+12.03896 g:17.748 r:16.317 i:15.115 z:14.495 g–r:1.431 r–z: 1.822
Star 3: RA: 239.99218 DEC:+12.01587 g:16.821 r:16.511 i:15.881 z:15.781 g–r:0.706 r–z: 1.040

FIGURE 3: Results from a test showing the influence of DCR in a red filter on very red stars. The data were obtained with the Liverpool telescope on La Palma (Spain) and RATcam. The left panel shows the field and indicating the red star and another star used for comparison purposes. The upper right panel shows the Right Ascension plotted vs. the hour angle for the red object, and the lower one the comparison star. Positions and magnitudes are given below the actual figure. The trend of RA with HA is clearly visible in the upper plot.

and V it is much larger and largest of all in B. NIR detectors are still not a widely available, and often either their pixel scale is too coarse, or the FOV too small, in many cases both. Therefore using NIR is currently not an option for the bulk of GBOT observations. Using the I band was considered by GBOT, and from the standpoint of making the need to correct for DCR as small as possible, it would almost be ideal. However, the I-band features several other drawbacks, which made GBOT decide to use the R-band. Firstly, most CCDs tend to be less sensitive in I band since their curve of throughput is already closing in this wavelength range. Then the sky background levels are significantly higher than in R-band, leading to very much decreased S/N. Since GBOT needs to get short exposures of faint *and* moving objects, this is a major drawback. Moreover, the skylines in this passband cause an effect known as fringing; while this can usually be removed, doing so adds even more noise, thus further decreasing the S/N of objects. For these reasons the I band imagery is usually much less deep than the other passbands in most multi colour surveys. The loss of depth can be more than 1 mag. For these reasons GBOT has chosen to focus on the R-band as a compromise, keeping in mind that correction for DCR is much more important than when using redder bands.

Several studies have attempted to measure the magnitude of DCR and to develop countermeasures. One method would be to take images of the field at a large hour angle, i.e. images in which the DCR effect is very pronounced and use these to determine the relations. Such methods are used by e.g. Costa et al. (2009) and Méndez et al. (2010). For GBOT and its modus vivendi of using very limited amounts of telescope resources this method is in general no option, since this would imply the need of revisiting the Gaia-field several times per night. Moreover these studies aimed at precisions/accuracies in the order of 2 mas, thus a much higher level of accuracy as GBOT. For these reasons, we need to apply an numerical solution, similar to the polynomials obtained by Monet et al. (1992) or Jao et al. (2005). Stone (2002) studied the influence of DCR in several passbands using real stars[4], and developed a model for black body and spectral templates. It appears that in general the blackbody DCRs and those of stellar templates are mostly quite similar for most of the colour range, however for very red stars the two relations start to deviate, especially (alas) in the R passband. This becomes apparent at $B - V > 1.5$ mag, corresponding to about M2-3 for dwarfs, M0 for class III giants, and K7 for class I giants. Therefore the prudent course of action would be to avoid using stars with $B - V > 1.5$ mag wherever possible - since they are either very intrinsically very faint or rare, they are not very common in the magnitude range exploited by GBOT. This presents us with two difficulties, the first being that in the initial phase we cannot assume to have precise[5] colour information about the background stars - in fact this will be mostly not the case. Fortunately this problem will be solved in the second (and any additional) iteration since Gaia will provide us with the necessary information. The second one would be that a star meeting this criterium might actually be crucial for the astrometric solution, if, e.g. a field is very empty. Therefore we need to extend the numerical relation to red colours as well. In the range of $-0.3 < B - V < 1.5$ mag, the total

similar filters in other filter systems, such ad Gunn, Vilnius, Bessel, SDSS, etc.

[4]testing the wide passbands against images taken in a H_α line filter, which per definitionem has no DCR

[5]non-photographic - most stars at current have photographic magnitudes coming from the POSS or other sources

range of DCR at a zenithal distance of 45°in the R passband will according to Stone (2002) (see his Fig. 5) 60 mas, in the region $B - V > 1.5$ mag alone, it adds another 40 mas. The same behaviour is also present using the I filter, just on a much lower scale. Here the blue part of the DCR spans about 18 mas, with the red tail adding another 8 mas. This range of 60(100) mas in R is of course not the residual error, this would be the maximal error if not corrected for DCR. When corrected, the residuals should be much less, one should aim at less than 5 mas. A good way to correct for DCR is to calibrate against a colour, such as $R - I$. In this case the residual intrinsic scatter will be in the order of 6 mas (Monet et al., 1992), Jao et al. (2005) cite a scatter of 5-9 mas. Monet et al. (1992) were able to obtain parallaxes with a mean error (of their sample) of 1 mas, using a polynomial for the correction of DCR. Since more than just one star will be used, this scatter (which also includes the centroiding error) does not mean that this is the DCR induced error of the stellar coordinate grid, which will be significantly smaller. It needs to be kept in mind, that colour information will only be available after the first release of Gaia photometry. Additionally, Monet et al. (1992) state that the influence of ambient pressure and temperature should *not* be underestimated; these quantities can produce an error in the DCR correction of up to 15%. One should also take into account, that the colour range of most field stars is not as large as it could be in principle (e.g. blue stars and (see above) very red stars are quite rare). Furthermore stars of different colours will be mixed in most fields, therefore the astrometric reduction will to a certain extent even out the offsets of the stars from their nominal position. This will also help minimising the effect of DCR on GBOT observations. Problematic will be scarce fields.

Finally the question would be the colour of Gaia itself. Of course, at current we have no knowledge of this quantity, which as time proceeds can and most likely will, also change. However we do know the colour of the light source illuminating the spacecraft, namely the Sun. And, assuming that the reflective nature of the Kapton material and other surfaces of Gaia will not completely differ from Planck, for which we have colour information obtained with the multi passband images GROND and the 2.2m telescope on La Silla, Chile. Its $g - r$ index is ~0.65 and its $r - i$ is ~ 0.23 mag[6].

In order to accommodate for DCR the following measures are suggested:

- DCR should be corrected via a previously derived polynomial, similar to those of Jao et al. (2005) and Monet et al. (1992). Since we will be using different filter systems (we have to take what we get offered by the partner observatory), e.g. Johnson-Cousins (J.-C.) or SDSS, these fits should be derived for every telescope system. We will not consider changes of transmission due to aging of the filter, or detector, buildup of dust, etc.
- The colour of Gaia, and possible/probable changes need to be tracked and quantified. This should preferable be done using a simultaneous instrument, such as

[6]Due to the overlapping nature of the Johnson-Cousins passbands, simultaneous cameras like GROND or BUSCA cannot use this photometric system. SDSS, Gunn and Stroemgren systems work

GROND (ESO-La Silla) or BUSCA (Calar Alto Spain). The reason for this is to exclude rapid variations as experienced in the cases of WMAP and PLANCK. Unfortunately measuring the colour in J.-C. filters simultaneously is not feasible, since these passbands overlap. Here we will have to take advantage of conversions between e.g. SDSS and J.-C.

The residual error depends on many variables and is not easy to quantify. However given the experience of other studies, for a well populated field, and not using extremely red stars, as well as assuming that Gaia will not have extreme colours, the residual effect of DCR should be limited to significantly less than 5 mas. A study using data from the Liverpool telescope is underway to evaluate the influence and correctability of DCR, and in a future version of this document, this will be included.

2.1.3 Relativistic light deflection

According to the general relativity (Blau, M., 2012), the gravitationnal bending of light (deflection angle α) by a body of mass M and radius R is given by

$$\alpha = 4\frac{G \cdot M}{R \cdot c^2}$$

where G denotes the universal gravitational constant and c the vacuum speed of light. This value is twice the value given by the Newtonian theory (Coles, 2001). The numerical values for G and c are:

$$G = 6.67384 \cdot 10^{-11} m^3 kg^{-1} s^{-2} \text{ and } c = 299792458 \text{ m}\dot{\text{s}}^{-1}.$$

For the moon (i.e. for a light ray that grazes the lunar limb) $R = 1.7374.10^6$ m and $M = 7.3477 \cdot 10^{22}$ kg which gives us a value for the deflection angle of

$$\alpha = 1.26 \cdot 10^{-10} \text{ rd} = 26 \mu\text{as}$$

(see also Crosta & Mignard 2006).

This value can be considered negligible at the 10 mas precision level of GBOT.

2.2 Astronomical effects

2.2.1 Atmospheric effects

This section deals with the more transient atmospheric effects, i.e. those that are subject to significant change on a nightly or even sub-nightly basis, such as lunar phase, sky transparency, seeing. Refraction has it's own section, since it is a principle property of the atmosphere, does not change by that large amount, and is of so large importance for the subject of this document, that this merits an own section.

1. **Seeing** Seeing is a specific type of small scale refraction variation, causing a degradation of optical images and a loss of optical resolution. This loss of resolution is not significant for GBOT, since we are not aiming at resolving objects close to another. A certain amount of seeing is actually beneficial, since one needs a certain sampling of a point spread function over the detector's pixels to properly centroid a source. For this reason we have introduced a lower limit to the instrumental pixel scale of $0.4\times$ median seeing. To much seeing on the other hand degrades the overall S/N ratio of an image, since the PSF is smeared over more and more pixels. Thus observations obtained under bad seeing conditions are less deep than those obtained under better conditions. Overall seeing is almost entirely a precision effect, and does not present any systematics. As a measure to counteract bad seeing conditions would be to increase exposure time, which is also facilitated by the fact that the signal of object motion is also blurred and our target will stay reasonably round for longer. If the seeing is too bad, the data should be discarded. Overall, seeing doesn't add to the budget of systematic errors, but depending on its magnitude it increases the r.m.s. error of a measurement.

2. **Transparency** Obviously, the transparency of the sky affects the depth of observations. Therefore observations should only be conducted, when the sky is reasonably clear. Presence of clouds should be noted, so that this information can be brought into consideration during the reduction and analysis process. Small scale transparency variations, e.g. high profile cirrus or other contrasty clouds, can have an effect on the timestamp accuracy. Apart from this, the influence of transparency and its variations does not have a significant influence on the accuracy, but of course on the precision of a measurement. Unlike in the case of seeing extending exposure times is not an option for counteracting bad transparency, since the object PSFs themselves are not altered by this, and a moving object will become elongated irrelevant of the ambient sky transparency conditions.

3. **Lunar phase** The moon illuminates the sky, causing a higher background level (the same applies to other, e.g. artificial but also polar light, sources illuminating the night sky.). The sky background is detrimental for the S/N, i.e. depth of astronomical observations, and depth is one of the most important parameters in GBOT

observations, since we are observing a moving, faint object with small telescopes featuring small fields of view, leading to a limited number of mostly faint background reference stars. For this reason we chose to observe using a red passband (i.e. R, r), rather than an OIR one (i.e. I, i) , despite having to deal with a much larger amount of differential colour refraction. Unfortunately the sky background rises dramatically, once reaching full moon. Moreover, in the worst phase, i.e. Full Moon, the Moon is actually near the L2, i.e. in the vicinity of Gaia. This results in monthly gaps in the coverage of Gaia of about 3 days. The adjacent days will also have their data quality diminished somewhat, the exact amount still needs to be established. Fortunately, the further away from Full Moon, the less bright and the further away from our target Earth's satellite will be, limiting the influence of Moon induced sky brightness for the largest period of time significantly. Other sources of sky brightness are polar lights (very rare effect, which will be increasingly less likely to happen, as we move away from the solar maximum, expected to be in 2013), artificial lighting (hopefully will only have a minor influence, since we are using observatories in remote, dark sites), etc. Overall, again this effect mostly has an impact on the precision rather than the accuracy.

2.2.2 Stellar densities

The L2 region and thus the location of Gaia moves through almost the full scope of galactic latitudes, and therefore an enormous span of stellar counts in the fields. Round about winter solstice the L2 almost coincides with the Galactic centre, during spring equinox it is high in the north polar cap, and 6 months later high in the southern polar cap. This means, that especially round the equinoxes, i.e. when GBOT observations are most important, stellar densities tend to be low. This presents itself as a problem, especially in the case of smaller field of views. For this reason, we placed an lower limit for field size around 5'×5'[7]. Larger, e.g. 10'×10' detectors will not as much suffer from this problem, but in some cases even then, the stellar coverage of the field might be sub-optimal. This especially holds true, if a large part of the FOV is completely blank, or only with covered by one or two stars. In these cases a proper astrometric reduction cannot be done, and in some cases the pipeline software does not reach a result. In any case in a field with only a small number of stars the order of the fit is limited, in many cases to linear only. As seen in the description of various other effects in this document, this may not be enough and residual systematic effects may remain. In some cases this can be overcome (see e.g. Sect. 2.1.2.2) by "manually" correcting for said effect. In the most extreme cases, data may need to be discarded. It remains an ongoing task for the GBOT group to develop methods limiting the amount of rejects[8]. The magnitude the sub-optimal astrometry resulting from sparse field astrometry is hard to quantify, therefore a solid number of how much this contributes to the overall error budget is not prudent.

[7] since this FOV also coincides with a decent pixelscale when using the widespread 2,048×2048 pixel arrays
[8] this should also be addressed in the GBOT meeting in Torino

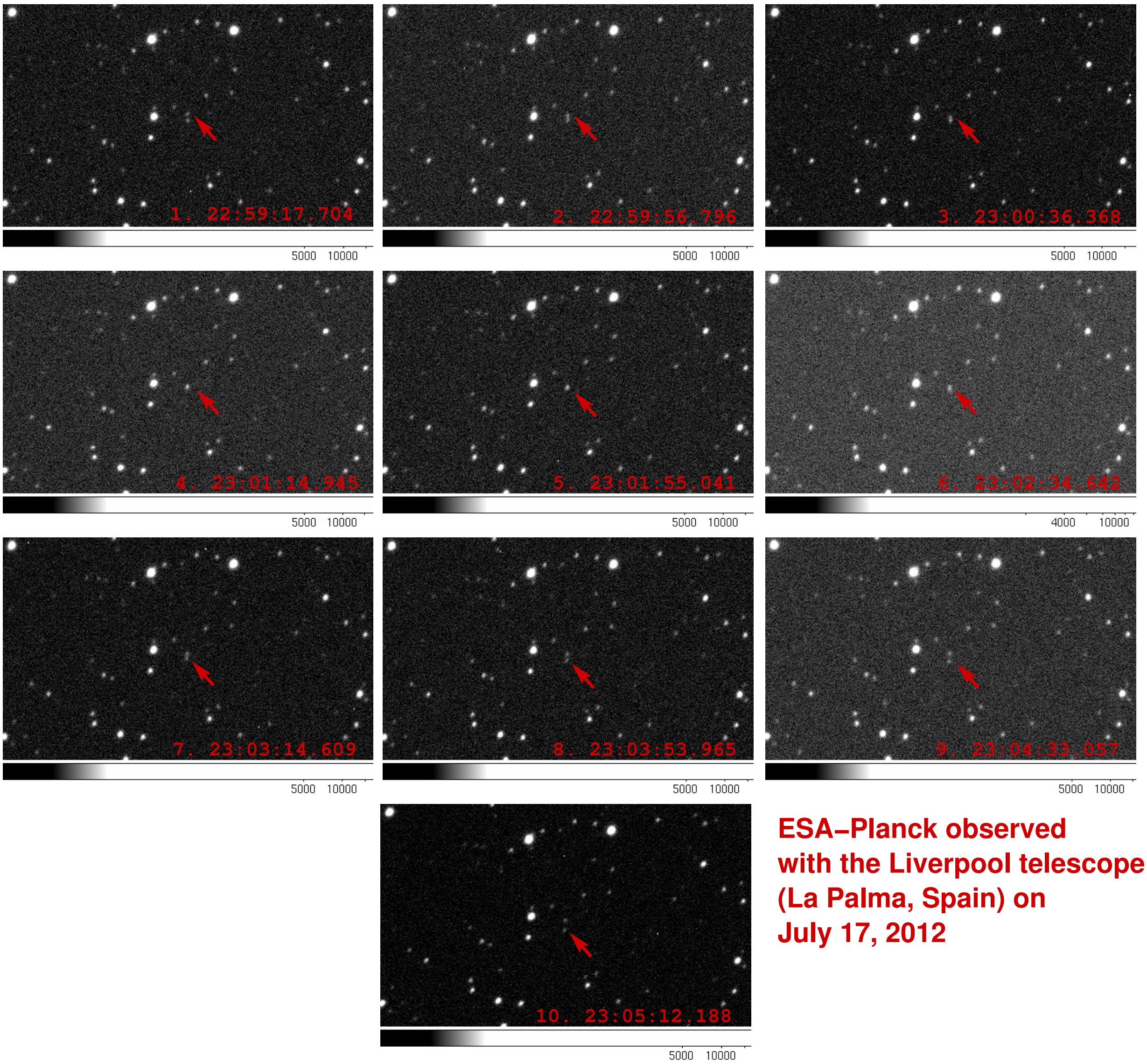

FIGURE 4: Sequence of observations of the Planck satellite taken with the Liverpool telescope on July 17, 2012. During these observations the satellite unfortunately crosses a background star in this moderately dense field. While statistically rare, these events will occur, especially in the more dense stellar environments when the L2 passes the Galactic plane in December-January and June-August. The consequence of such an occurance is, that the data is partly lost (in this case 4 out of the 10 images will be useful). It is foreseen to establish a pre-warning system based on the ephemerides.

In contrast to sparse fields, dense fields also present a significant amount of challenge to GBOT data taking. While in principle, the more stars are available the better the resulting astrometric reduction will be, since one have ample star coordinates everywhere and higher order polynomials at one's disposal. Here, the devil lurks in the detail. One problem (not necessarily restricted to dense fields) would be that the target object, i.e. in our case Gaia (or Planck) would be transversing another object. If this object is bright enough, the workaround would be to inform observers about this issue and to tell them not to observe during the time the two objects are to close together. How practical this approach actually is, will have to be tested; here is one thing that is presumably much easier to accomplish with facilities having a human observer, rather than being robotic. It will be the task of the GBOT member on duty to look for such conflicts and issue warnings to the observers to whom this applies. What remains are those stars too faint to be evident on the finding chart. Of course their effect on the coordinate will be much less than those of brighter objects, but this does not mean, it is going to be negligible. At the moment there is no workaround for this, hopefully the effect of the interloper will be seen in the results, so that the affected frames can be discarded. For this the sequences need to be long enough to ensure unaffected frames.

Fig. 4 shows a sequence of test observations taken with the Liverpool telescope using the Planck spacecraft as a target, during which the satellite crosses a background star of similar magnitude. In the worst case such observing sequences will be useless, and will have to be discarded. This will be a very rare occurance, since there are only about 100,000,000 stars as bright or brighter than R=18 mag. Nonetheless it is planned to set up an automated warning system for observatories, issuing warnings about stellar sources lying ahead on the track of the satellite[9]. Potentially more harming could be fainter stars, which are not readily recognised, yet bright enough to interfere with the centroiding. Here only a consequent and strict Quality Control will help.

Dense fields also mean some degrees of crowding, i.e. star overlapping each other. These will have detrimental effects on the quality of the coordinates of such objects, and may lead to accuracy problems in the astrometric solution. For most cases such objects could be weeded out by filters looking at their overall shape, i.e. effects such as ellipticity, FWHM, etc. This way, galaxies and other extended objects may be culled from the list of stars as well.

The potential problems induced by dense fields are in general not quantifiable, but in most cases may be circumvented by relatively simple methods. Therefore dense fields are overall expected to less problematic than sparse fields.

2.2.2.1 An analytical approach to determine magnitude of influence of faint star signals overlapping with the satellite PSF The case of the target object transversing another source of similar brightness or brighter than itself, i.e. the case described in the previous part is easy to

[9]This will probably not be available at the start of operations, since this is not the highest priority item.

handle: The according files will be discarded and not used. The same will apply in the situation that the offending object is significantly fainter than the target, but still bright enough to be noticed. More problematic are those instances where (and this will happen frequently in areas of high stellar density), where the obstacle is very much fainter than the moving source and maybe even not obvious to visual inspection. In order to estimate the constraints on this, we have analysed this scenario analytically. This analysis is somewhat similar to those of the sky gradients, see Sect. 2.3.1.

We start off with signals of two stellar sources, with the first one, S_1 being the moving source, and the second one, S_2 that of a background star. S_1, i.e. the moving source is significantly brighter than S_2:

$$S_1 = a_1 \cdot e^{-\frac{(x-b_1)^2}{c^2}}; S_2 = a_2 \cdot e^{-\frac{(x-b_2)^2}{c^2}} \tag{9}$$

We assume that the FWHM of both sources, given by c is equal, i.e. both are point sources. Furthermore $\Delta b = b_1 - b_2$ is small. It is clear that the question whether an interfering signal alters the position of the prime object to a noticeable degrees depends on two parameters, a_1/a_2 and Δb. The total light spread function is now:

$$S = S_1 + S_2 = a_1 \cdot e^{-\frac{(x-b_1)^2}{c^2}} + a_2 \cdot e^{-\frac{(x-b_2)^2}{c^2}} \tag{10}$$

Next, we form the first derivative to determine the local maximum/extremum[10] which will be zero at the location of the minimum:

$$\frac{dS}{dx} = -a_1 \cdot \frac{(x-b_1)^2}{c^2} \cdot e^{-\frac{(x-b_1)^2}{c^2}} - a_2 \cdot \frac{(x-b_2)^2}{c^2} \cdot e^{-\frac{(x-b_2)^2}{c^2}} = 0 \tag{11}$$

Developing the bell function part as a taylor series around $\Delta b_i = x - b_i$ gives us:

$$\frac{dS}{dx} = -a_1 \cdot \frac{\Delta b_1^2}{c^2} \cdot (1 - \frac{\Delta b_1^2}{c^2}) - a_2 \cdot \frac{\Delta b_2^2}{c^2} \cdot (1 - \frac{\Delta b_2^2}{c^2}) = 0 \tag{12}$$

$$\Rightarrow a_1 \cdot \Delta b_1^2 \cdot (1 - \frac{\Delta b_1^2}{c^2}) = a_2 \cdot \Delta b_2^2 \cdot (1 - \frac{\Delta b_2^2}{c^2}) \tag{13}$$

Assuming that the shift in position caused by the merged faint object is significantly smaller than the FWHM of the PSF, i.e. $\Delta b_i^2/c^2 << 1$, one can simplify this equation to:

[10] Since we know, that we are looking for a maximum, given that both signals are positive, we do not need to form the second derivative as well.

TABLE 2: Numerical table showing the offsets of the combined maximum in respect to the centroid of the undisturbed signal of the prime source in dependence of the flux ratio of the two objects and the locus of the secondary. Please note that we have made assumptions and simplifications in the analytic approach, as shown in the text. Therefore the values get less and less accurate for larger b_2, since these assumptions get less and less justified (see text)

	b_2 in units of c								
a_2/a_1	0.1	0.2	0.3	0.4	0.5	0.6	0.7	0.8	0.9
0.001	0.0001	0.0002	0.0003	0.0004	0.0005	0.0006	0.0007	0.0008	0.0009
0.005	0.0005	0.0010	0.0015	0.0020	0.0025	0.0030	0.0035	0.0040	0.0045
0.01	0.001	0.002	0.003	0.004	0.005	0.006	0.007	0.008	0.009
0.05	0.005	0.010	0.015	0.020	0.025	0.030	0.035	0.040	0.045
0.1	0.01	0.02	0.03	0.04	0.05	0.06	0.07	0.08	0.09
0.2	0.02	0.04	0.06	0.08	0.10	0.12	0.14	0.16	0.12
0.5	0.05	0.10	0.15	0.20	0.25	0.30	0.35	0.40	0.45

$$a_1 \cdot \Delta b_1 = a_2 \cdot \Delta b_2 \tag{14}$$

Solving equation 14 for x, one arrives at:

$$x = b_1 + \frac{a_2}{a_1} \cdot b_2 \tag{15}$$

For reasons of simplification we make the following coordinate transformation, centring on the locus of the moving object:

$$x' = x - b_1 \tag{16}$$

$$\Rightarrow x' = \frac{a_2}{a_1} \cdot b_2 \tag{17}$$

Since this result depends on two parameters, namely a_2/a_1 and b_2, we have to continue numerically from here. The results are shown in table 2.

Our result, and thus the values given in table 2 also have an implicit dependency on the FWHM, i.e. c, or in more practical terms, the seeing. Assuming, e.g. a c of 1”, one can easily see that a secondary object with more than 1% of the target flux will noticeably affect our measurements, and 5% and more will render them useless.

The above is only valid, if the difference in position of the two objects is significantly smaller than c, allowing us to make the simplification in equation 13. For Δb significantly larger than c, the signal will eventually split up and have two maxima, one for the target and one for the secondary. For a certain range these will still be affected by each other, less and less as the distance increases. The most problematic region is when the distance becomes similar to the seeing value, when things become complicated analytically and cannot so easily be solved. This also has consequences for the values of the rightmost columns of table 2, meaning that the true values will start to deviate significantly from the calculated ones, as given in this table. However the general conclusion that images where an interfering object is brighter than 1% of the target should be treated with care, and those with more than 5% should be discarded will most likely still hold true.

Finally, one should also note, that there is an influence of the centroiding method on the effect an interfering source has on the coordinate, especially if the two sources are further apart than the seeing radius. Obviously, using the barycentre method is more prone than other, more sophisticated methods. The GBOT pipeline is equipped with several algorithms, and should be less affected. Nonetheless the results from this section apply also for data reduced by the GBOT pipeline

This means that images will need to be inspected whether there is a faint object passing the trajectory of the target, and discarded if necessary.

2.2.2.2 Cosmic ray imprints, satellite trails, etc. Apart from fixed objects, such as background stars or galaxies, an image can also be blemished by a satellite trail (other than the target of course) or cosmic rays. The former is easily seen, and in the rather unlikely event that the trail overlaps the target[11], the image should be discarded. If one of the reference stars is affected, that star will be excluded. Unfortunately most cosmic rays signatures affect only one or a few pixels (but with high intensity) and in many cases a cosmic ray superimposed on a star signal is easily overlooked on visual inspection. Fortunately, because of the very high flux level (even up to saturation), most centroiding methods will either fail or give large error margins, or a result strongly deviating from the others in a sequence; allowing the affected image to be discarded. Again, such events will not be common, especially since our exposure times are short. However experience shows that this will happen a few times. Should a reference star be affected: there is not straightforward way to exclude it from the solution, since visual inspection of every star on an image is far too time consuming - the only viable method is to discard frames with bad or deviant astrometric results.

2.3 Optical and detector effects

Elimination of optical effects are the core problem of any astrometric reduction. This can either be done by explicitly compensating for the effects themselves or by fitting a 2D-polynomial so that all effects are compensated. In theory this means that after the astrometric reduction the optical effects, such as defocus, astigmatism, spherical and chromatic aberration[12], coma, field

[11] On the other hand, Murphy's law applies here too!
[12] not to be confused with the relativistic aberration, which is an entirely different effect!

curvature, distortion etc. are fully compensated, but especially if the star density of the field is very low limiting the order of the polynomial fitted to the data, some residuals may remain. These residuals are principally quantifiable, however this requires a significant effort, which is not feasible on a daily basis. However the astrometric properties of each participating facility needs to be monitored. A precise procedure for this still needs to be established.

Also in this category are all issues concerning the detector, which nowadays is mostly a CCD-semiconductor array. Potential problems could be the error of the pixel size, and especially for front illuminated systems, in which the gating electronics sits above the pixel, thus in the way of the light, the pixel structure. Most newer CCDs are back illuminated, they therefore feature a much cleaner less obstructive surface, which in principle should yield more accurate results for both photometry and astrometry - however to our knowledge an attempt to verify this has not been tried. A downside of thinned back illuminated CCDs is the occurance of fringing at longer wavelengths, noticeably from I/i passbands on. Another issue connected with the CCD detector is the pixel size itself[13], which needs to fulfil certain minimum requirements (specified in the list of GBOT requirements) to achieve proper sampling, thus fully allowing to access the precision, without special measures such as drizzling methods (e.g. those used to extract sources from HST data), which GBOT does not plan to invoke.

2.3.1 Sensitivity variations and illumination gradients across the field

No astronomical image is perfectly illuminated over its entire field. There are several effects preventing this from happening. In the following the influence of those will be estimated and described. 2D-variations in the effectivity of light being recorded can have several causes:

1. The optics can have field dependent throughput. This is especially true when focal reducing systems are used, which quite often have a visible amount of vignetting. Also dust on filters, CCD entry windows, etc. can affect the efficiency in which infalling light is lead to the detector.
2. The detector itself has a variable efficiency in which it can register incoming photons. Mostly this is caused by processing artefacts, either originating in the production of the chip or in the thinning process. Fortunately modern back illuminated thinned CCDs have less blemishes than earlier generations. These variations are mostly on a pixel-pixel scale or at most comprises 10's of pixels in one coordinate.
3. Stray light, light leaking into the optical system from the outside can cause an additional additive gradient. For detectors cooled to less than -100°C the on chip amplifiers can add an additive signal. The problem is, that these additive gradients are hard to be distinguished from those multiplicative ones, described under point 1 in this list. In many cases it is not even possible to completely separate the two.

[13]or actually the pixel scale, i.e. the angle in the sky each pixel covers

These three effects will be discussed here and their consequences, if any, evaluated.

2.3.1.1 Large scale gradients In principle there are two effects to be discussed here, one being an additive background gradient, the other a multiplicative one.

The first type, which adds an additional large scale background signal, does not alter the source signals on the image as such. This means that the count rate per pixel coming from a source will stay the same with or without the gradient, the total count rate for a given pixel just gets increased by the count rate of the gradient - rather similar to the bias/dark level in untreated CCD images. Depending on the slope of the gradient, the centroid of a source (here we speak about gaussian PSFs of point sources for reasons of simplicity, in principle everything said here applies to other objects as well), can be altered by this large scale gradient. The cause of such a large scale additive signal can be stray light, especially if the moon is up, thermal effects, such as the heating effect of an on-chip amplifier, large scale ionised gas clouds in the sky itself, polar lights, etc. In photometry this effect is less harming than the multiplicative one, since the relative flux is conserved. It does however have an effect on the S/N, thus the error, which will be the case in astrometry too. Therefore it is very beneficial to have as few background signals as possible.

The second type, typically caused by bad or no flatfield correction, alters the flux of stellar sources. In other words, where the gradient is low, the count rates of stars in the vicinity are lower too, where it is higher, so are the countrates of stellar sources. For photometry this is potentially devastating, since the actual fluxes are changed significantly. For astrometry the detrimental effect is less obvious, since astrometry depends on the centroids rather than the total amount of counts. Again also the S/N is affected. Therefore care should be taken to perform a good flatfield correction.

In reality there are often residual traces of both effects, and it is not also straightforward to distinguish between the two. In the following we attempt an analytical solution of both problems, in trying to determine whether the locus of the maximum of a stellar source, represented by a Gaussian, shifts when subjected to either type of gradient, and if so, how much this shift would be. In mathematical terms, this is a classical maximum/minimum[14] searching analysis. This means, we have to compute the first derivative and find its zero points. Since we know that we are looking for a local maximum, there is no need to look at the second derivative. For reasons of simplicity the problem is reduced to a one dimensional one. The equation for the source looks like this:

$$S_0(x) = a \cdot e^{\frac{-(x-b)^2}{c^2}} \tag{18}$$

[14] in our case we are looking for the maximum

and the slope which will be added resp. multiplied to this source function:

$$S_g(x) = m \cdot x + n \tag{19}$$

This of course assumes that the underlying gradient is linear, which in reality it often isn't. However, one can make this assumption, since the patch of the field of importance is small, and one can thus safely assume that, since we are looking at *large scale* effects here, that the gradient is in fact linear.

2.3.1.1.1 The additive case First we create the full light function by adding equations 18 and 19, to get:

$$S_a = S_0 + S_g = m \cdot x + n + a \cdot e^{\frac{-(x-b)^2}{c^2}} \tag{20}$$

then form its derivative, which should be 0, in the case of an extremum, i.e. in our case a local maximum.

$$\frac{\mathrm{d}\,S_a}{\mathrm{d}\,x} = m + a \cdot \frac{(x-b)}{c^2} \cdot e^{\frac{-(x-b)^2}{c^2}} \equiv 0 \tag{21}$$

We now get rid of the $x - b$ term (in principle by changing the coordinate system from the image system to one centred on the original position of the source) by:

$$x = b + \Delta b \tag{22}$$

which now simplifies equation 21 to:

$$m + a \cdot \frac{(\Delta b)}{c^2} \cdot e^{\frac{-\Delta b^2}{c^2}} \equiv 0 \tag{23}$$

Since we can safely assume, that the change in maximum induced by the gradient is small, we replace the exponential function by its Taylor series, limiting this to 1st order to arrive at:

$$m + a \cdot \frac{(\Delta b)}{c^2} \cdot (1 - \frac{\Delta b^2}{c^2}) \equiv 0 \tag{24}$$

Furthermore assuming that the shift Δb is significantly smaller than the FWHM of the PSF, the term $\frac{\Delta b^2}{c^2}$ becomes even smaller when compared to 1, which leads to the result of:

$$\Delta b = \frac{m \cdot c^2}{a} \tag{25}$$

This means that (in the realm of arcseconds) for Δb to stay below 10 mas or 0.01”, $m < \frac{\Delta b \cdot a}{c^2} = 1N/''$ for a star with $a = 100$ counts, or $m < 0.5/''$ for a star with $a = 50$ counts. Over a field of 10’ 1 count per arcsec means 600 counts. Such large gradients are rather unusual. Furthermore, since all stars are affected (assuming that the gradient is not too off linear) in a roughly similar way, the differential shift, caused by non-linearities in the gradient are even smaller. Therefore it is safe to assume that an effect caused by additive gradients on the results is negligible, unless something went very wrong; usually such data will be discarded. As a word of caution, it remains to be seen, if this all also holds true for data obtained during full moon, where large gradients are to be expected. Additionally one should mention, that of course any additional unwanted light signal adds its own noise, and thus reduces the S/N of the observations. Therefore while the systematic effect on the accuracy of the extracted coordinates in the presence of an additive gradient can be neglected in most cases, this does not hold true for the impact on the precision.

2.3.1.1.2 The multiplicative case Again, we start by creating the full light function, this time by multiplying equations 18 and 19, to get:

$$S_m = S_0 + S_g = (m \cdot (x - b) + 1) \times a \cdot e^{\frac{-(x-b)^2}{c^2}} \tag{26}$$

then form its derivative, which should be 0 in the case of an extremum, i.e. in our case a local maximum.

$$\frac{\mathrm{d}\, S_m}{\mathrm{d}\, x} = m \cdot a \cdot e^{\frac{-(x-b)^2}{c^2}} - (m \cdot (x - b) + 1) \cdot \frac{(x - b)}{c^2} \cdot e^{\frac{-(x-b)^2}{c^2}} \equiv 0 \tag{27}$$

We now get rid of the $x - b$ term (in principle by changing the coordinate system from the image system to one centred on the original position of the source) by using equation 22, resulting in the following simplified version of equation 21:

$$m \cdot a \cdot e^{\frac{-\Delta b^2}{c^2}} - (m \cdot \Delta b \cdot \frac{\Delta b}{c^2} \cdot e^{\frac{-\Delta b^2}{c^2}} \equiv 0 \tag{28}$$

As in the previous case we can safely assume, that the change in maximum induced by the gradient is small, we replace the exponential function by its Taylor series, limiting this to 1st order to arrive at:

$$m \cdot (1 - \frac{\Delta b}{c^2}) - (m \cdot \Delta b + 1) \cdot \frac{\Delta b}{c^2} \cdot (1 - \frac{\Delta b^2}{c^2}) \equiv 0 \tag{29}$$

Furthermore assuming that the shift Δb is significantly smaller than the FWHM of the PSF and the slope of the gradient is also locally small, the term $M \cdot \Delta b$ can be neglected, which leads to the result of:

$$\Delta b = m \cdot c^2 \tag{30}$$

This time the shift does not depend on the amplitude of the PSF, only on its breadth and the slope of the underlying multiplicative gradient. Assuming the former to be 1", and the tolerance in shift 10 mas, the slope should be less than 0.01/arcsec or 1% per arcsec. This could theoretically be problematic, since good even good flatfielding often yields a residual gradient of 1-2%. However, since, given a rather simple 2D structure of this gradient, will lead to all sources shifting in similar directions, leading to a general shift, which is totally without significance, and minor residual shifts, resulting from the gradient not being entirely linear in all places on the field. In this multiplicative case, even the brightness of the source does not play a role. Again, all extra unwanted signals do present an additional source of noise.

2.3.1.2 Mid-scale structures In most cases, these will be multiplicative in nature, often being caused by dust specs on a glass surface relatively near the focal plane or even on the chip itself, as well as artefacts on the chip, which were quite frequent for older devices. These intrinsic CCD structures have rather sharp borders, the shadows of dust specs are blurrier, depending on the focal ratio of the system an the distance to the focal plane. If they are far away from the focal plane, and in systems with a large focal ratio, they almost merge into the general large gradient, increasingly becoming large scale gradients themselves. The typical size of the structures dealt with here are 10s to about 200 pixels.

In principle the same applies, as said about the large scale gradients in the previous section. However all of the assumptions and simplifications made there are no longer valid. It is to be assumed, that especially PSFs lying on the border of such a structure will be severely affected. It will be difficult to quantify the impact of these mid-scale structures on the centroid of a PSF, given the diverse size and shapes of these artifacts. Since these effects can be easily accounted for in the flat fielding process, and usually vanish completely if the flat fielding is done properly, a strict treatment of these structures is futile. Images showing significant residua of such blemishes, will be discarded.

2.3.1.3 High frequency effects, pixel to pixel sensitivity variations No CCD-Array is perfect, every single pixel has its own response and sensitivity characteristics. Some pixels are even completely insensitive, these are called bad pixels, or depending on their count level as hot or cold pixels. Furthermore some bad pixels block the reading out of a complete row, so that the information in the remainder of the -as such perfectly good - pixels of the affected row, gets lost, this is called a bad row. There are routines to cure bad pixels or rows, usually be some kind of interpolation and adding of the correct amount of noise. The results of this type of correction are quite good, stellar images treated this way even deliver acceptable results for positions. However, GBOT will *not* use stellar images affected by a bad row, therefore a bad pixel mask must be available, so that all bad regions can be masked out with liberal margins at the borders of bad areas. Stars located within these zones, will not be used for the astrometric solution, and if the target objects is affected, the whole frame should be discarded.

Apart from defects, every pixel has a slightly different sensitivity. Of course, the overall sensitivity of a given pixel depends on more than the pixel itself, but also on the optical lightpath illuminating a particular pixel. However the effects caused by obstructions in the optical lightpath are usually larger than pure pixel to pixel variations, and are described in Sect. 2.3.1.2. For most chips, especially those with adequate cooling, the pixel to pixel variation is small, and mostly overwhelmed by the ambient noise. For this reason, we do not expect significant effects , especially when the object is well exposed, i.e. has a sufficient S/N. For faint objects one can expect an effect, which is at current being analysed, and will be presented in a future edition of this note. That said, it is important to note, that most if not all of such pixel to pixel variations are compensated by the flatfield correction, therefore under normal conditions we do not expect much negative influence from these high frequency signatures. In order to put weight on this statement, we point to the analysis of the ESO-VST data MA-005, which was conducted on undetrended data, and gave us a $\sigma(O - C)$ of 20 mas and less, one of the best measurement sequences so far. If there would be a significant influence of the (uncorrected) small scale chip structure, the would have manifested itself in the form of an increased scatter, since the target (i.e. Planck) moved several 10s of pixels during the sequence.

2.4 Object centroiding, PSF

The first thing to consider and the basis of all good astrometry and photometry is the source extraction and centroiding. The stellar point spread function (PSF) is roughly a 2D gaussian distribution. Since our target is moving, its PSF has a certain amount of elongation, which is detrimental for the precision in the direction of movement. Therefore we keep exposure times short. There are a number of centroiding methods ranging from simple determination of the barycentre to full PSF fitting, as done by DAOPHOT (Stetson, 1987). Our pipeline has a set of options, such as Sextractor (Bertin & Arnouts, 1996) and its X, Y_{window} method to fitting a moving gaussian (optimised for moving objects). It is difficult if not impossible to compare these methods non-empirically, and an empiric approach shows no or very small differences in the results in dependence of centroiding method. Therefore one can say with quite a degrees of justification, that while centroiding is important, the method is far less critical than originally assumed. One would need to carry out more tests, especially in images with variable PSF.

2.5 Technical effects

2.5.1 Timestamp accuracy

This quantity does not affect the astrometry as such, but the subsequent orbit determination. For this reason this is also included in this assessment document. The relevant quantity here is the effective time of mid exposure[15], something which is not determinable with great precision, since this also includes changes in light throughput due to variations in the transmission (clouds!) and/or light amplitude variations of the object itself. Astronomical reduction programs, such as IRAF do allow to compute a quantity called the effective observing time; however this only incorporates the change in airmass - for the short exposures for GBOT the change in airmass during the exposure does probably not play a significant role. Therefore the formula for computing the mid exposure will stay:

$$t_{exp,mid} = t_{exp,start} + 0.5 \times T_{exp} \tag{31}$$

It should also be noted that not the clock accuracy is the crucial quantity here but the shutter time accuracy. Precise and accurate times can be obtained through various ways, such as atomic time signals (e.g. DCF 77 in Germany), the internet, GPS, etc. Therefore the *clock* as such will not be much of a problem in most cases, but one will also need to know the timespan elapsing between recoding the time signal and shutter opening and closing. A procedure of how to determine this still needs to be established.

Moreover, since a shutter does not close or open instantaneously, but as every moving object needs time to fully transverse the focal plane, the time of opening/closing of the shutter is not homogeneous. In case of the commonly used iris type shutters, this effect is negligible, since the opening/closing flanks of the window of exposure are symmetric, the first and last part of the aperture to be free is the centre and the edge is obscured longest both in opening. Of course this only applies if the opening and closing of the shutter is more or less identical (which it probably isn't). The situation is different with the modern door type shutters, which usually start at one side of the field and transverse to the other side. This means that the exposure window of one side of the aperture is earlier than the opposite side. Fortunately many of these shutters move very fast, which (hopefully) means, that shutter characteristics are not much of a concern, but this will need to be clarified with each telescope partner.

Overall, given the difficulties in a precise determination of this quantity, an accuracy of 0.1 sec

[15]This will *not* be the quantity given in the OPTO files, which will consist of the start time and the exposure time, from which the mid exposure will have to be computed

has been decided on as a compromise. Especially due to the effects outside of the telescope as such (sky or object variability), a tighter constraint is not feasible.

2.5.2 3D-Coordinates of the telescope

The telescope coordinates are related to the previous entry. With current GPS technology it is feasible to determine the telescope coordinates to an accuracy of less than one meter. The GBOT requirements are in the order of 7 m per coordinate. Since the measurement procedure for this has been described at length in **(insert citation)**, this will not be repeated here. Given that the expected error margin is much tighter than the required one, which already is set tight in order not to fill the entire error budget, the influence of properly measured telescope coordinates can be considered as negligible.

2.5.3 Reference catalogues

As in most astrometric procedures, the underlying reference material is of crucial importance. In our case, the influence of the reference catalogue will only be of significance while we have to use conventional mainly earth bound material. Once Gaia data is available, all existing observations will be re-reduced, and (of course) all new observations will be reduced, using this new and ultra-precise (and hopefully accurate) reference catalogue, which will diminish the influence of the reference catalogue on our results significantly. The GBOT observations will be reduced at least one more time after Gaia data taking has concluded, by then, with the full quality of the data, the signal of the reference catalogue on the whole error budget of GBOT will be negligible. However until then, especially in the initial period before the availability of Gaia data, this will be one of the main sources of error, in effect drowning many of the other more subtle influences described in this document. This also means that at current this document can only be regarded as preliminary.

Despite having significantly improved in recent years, deep astrometric catalogues have a variety of short-comings. Mostly they are assembled from using photographic plate material (for later epochs also CCDs or similar devices, either as tiles or as drift scans) projected in one way or another onto far less deep catalogues which are either based on meridian circle observations or space borne Hipparcos and Tycho astrometry. In general they are multi epoch catalogues, thus contain proper motions. In many cases the astrometry has been calibrated to an international reference frame, nowadays mostly the ICRF, i.e. to the extragalactic background, but some are not, e.g. the USNO catalogues. However all of them suffer not only from the statistic error (precision), but also from small to medium scale zonal error and from global reference frame errors.

The latter is in principle a global misalignment of the catalogue in respect to the reference grid of the e.g. ICRF, resulting in a tilt of the catalogue coordinate sphere in respect to the reference frame coordinate sphere. As with all inclined spherical coordinate systems the magnitude of the effect on the coordinates depends on the location on the spheres. However in practical terms this is not of much significance as long as one sticks to one catalogue, or if as common today, these misalignments are rather small. Nonetheless for the initial time, there might be a residual signal of this effect in the GBOT data, especially since it may become necessary to switch catalogues from time to time. With Gaia (which still will have a very minute reference frame error), this effect will not play any role whatsoever.

Much more harming, albeit again only in the earth bound reference catalogue era of GBOT, will be the small to medium scale zonal errors. These are mostly induced by the assembling procedure of these catalogues, namely using images (photographic or CCD, mostly both) covering a limited part of the sky, for each of which an astrometric solution needs to be found. These are then hinged into a global solution. Comparing any given set of two catalogues makes evident, that medium scale (10' - 2 degrees) residual zonal errors persist - these can be up to more than 50 or even 100 mas in magnitude.

Another issue with astrometric positions (this is true in all cases, even including Gaia data), is that the proper motion of stars obviously changes their position and the error of the proper motion accumulates on the error of the position. This means that the quality of positions degrades more and more the further away from the catalogue epoch the data are. As an example, for a proper motion error of 5 mas/yr and a positional error at the time of the epoch of 50 mas, the positional error will increase to 56 mas after five years, to 71 mas after 10 years and to 112 mas after 20 years! If the proper motion error is 10 mas/yr, the according numbers will be 71 mas, 112 mas and 206 mas.

It therefore becomes very clear, that this will be the overwhelming systematic effect on GBOT data before transiting to Gaia data. After that, the error of positions in the reference catalogue will be generally better than 0.3 mas, the proper motions (assuming a baseline of 5 years) will be better than 0.1 mas/yr for most objects. With a duration of the mission of about 6 years (nominally 5 years) the positional error at the end or beginning of the Gaia mission (i.e. at the extreme sides of the mean Gaia epoch) will be less than 0.5 mas, i.e. still negligible for GBOT purposes. However the final precision of Gaia will of course only be reached after all data have been collected. Earlier releases will have larger margins of error and will be less deep, which will have some impact on the quality on GBOT astrometry, but a much smaller one than the ground based data. The exact data quality of the first release of Gaia data is not exactly known, and at current holds several uncertainties, such as the date and scope of delivery. Reasonably, one can expect it to be overall similar to that of the Hipparcos mission, i.e. about 1 mas. This is not dramatic, but at least the missing depth of earlier releases warrant a third reduction of all GBOT data after the end of Gaia data acquisition, since especially in sparse fields, we need all available stars.

2.6 Miscellaneous effects

At current we have not considered any effects not fitting into on of the other categories above.

3 Total magnitude of the influence of the adverse effects on GBOT astrometry

As described in Sect. 2 our measurements are potentially affected by quite a number of effects, some of them very much depending on outer circumstances, such as field density, the instrumentation setup used, etc. Furthermore some effects may or may not be present entirely for a given set of observations. This makes it difficult to issue a robust and global estimation of an error budget caused by these effects. On the other hand, a significant number of the items of Sect. 2 are correctable and can be dealt with, invoking a fair amount of visual inspection and quality control. In some cases it might be better to discard an image, rather than mix bad data with good data. Thus the number of effects would boil down to maybe 4 or 5 that need to be looked at more closely, foremost the colour refraction and the reference catalogue quality which at current is the main limiting factor for the accuracy of our results. This will significantly change, after the astrometric reductions can be redone using Gaia data as reference catalogue. If all goes well, the now dominating factor reference catalogue in the error budget would essentially vanish entirely.

For this reason, we will give two estimations for the GBOT error budget, one for the situation before the first global solution and one for afterwards.

Table 3: Compilation of effects influencing GBOT astrometric results and their magnitude. The values given are the total magnitude of the effect, and the residuals before and after availability of Gaia reference catalogue data. In many cases letters are shown, instead of numbers, these mean: E - needs to be done by ESOC, P - effect on precision only, Not determinable, depends on situation, D depends on size of effect/deviation. This table is for reference only, for more details, please refer to the text.

Effect	Magnitude [mas]	pre-AGIS [mas]	post-AGIS [mas]	remark
Aberration				
–Annual	120,000	< 3	< 3	
–Diurnal		< 1	< 1	

Continued on next page

Table 3 – continued from previous page				
Effect	Magnitude [mas]	pre-AGIS [mas]	post-AGIS [mas]	remark
light time correction	E	E	E	needs to be corrected by ESOC
Refraction				
–Absolute	1,800,000	0	0	
–Differential	500 - 2000	< 5	< 5	can be corrected with linear term, if $h_z > 40°$
–Colour (DCR)	60 -100	5-10	~ 2	in R/r
Relativistic light deflection	0.26	0	0	negligible
Atmospheric effects				
–Seeing	P	P	P	
–Transparency	P	P	P	
–Lunar phase	P	P	P	near Full Moon precision will be low
Stellar Densities				
–sparse fields	N	N	N	impact on astrometric solution
–dense fields	N	N	N	merged stars, target moving over star
–Cosmic rays, trails, etc.	N	N	N	Affected images will be discarded
Optical/Detector effects				
–Sensitivity variations				
$\rightarrow$ large scale	D	D	D	usually well behaved, effect on all objects
$\rightarrow$ mid scale	D	D	D	good flatfield correction required, QC!
$\rightarrow$ high frequency	D	D	D	does not seem to present a significant problem
– object centroiding	< 50	< 5	< 5	dependency on method minor, only systematic effect accounted for
Technical effects				
–Timestamp	D	D	D	
–Telescope position	D	D	D	
Reference catalogue	up to 1000+	50-100	<0.3	

A compilation of the effects is given in Table 3. As one can easily see, most effects cannot really be assigned a general or global value for the size of its influence on the measurements. In general the impact of these will be relatively small, in some cases it really depends on a good data quality control. The main effects in the end are precision, differential refraction and DCR, the reference catalogues.

Precision is very much affected by the ambient conditions, such as seeing, sky transparency, sky brightness (especially lunar phase), but also object brightness and telescope/detector specifications - basically everything that has influence of the S/N of the target, but also the reference stars. Since the object is moving, extending the exposure time is only a very limited option. Increasing the number of exposures is a better option.

The two varieties of refraction also add significantly to the error budget. The differential kind, will be automatically taken care of with the astrometrical solution. If this solution is linear, the DR will be eliminated to a certain degrees, all observations with a horizon distance of more than 40°will be fine[16], for smaller fields such as our typical 5-10'×5-10' fields, even lower altitudes are possible. Therefore in most situations, this effect should also not present a significant problem. The differential colour refraction (DCR) is to be taken more seriously. There are way of correcting for this using a polynomial, however this depends on the object colour. For the reference stars, we will in the early phase only have a rough (based on the currently available photographic magnitudes) value for star colours in most part of the field. In some parts, data from the Sloan Digital Sky Survey or similar surveys may be available. But in General we will not have good knowledge about the colours of the background stars. However this will dramatically improve with the availability of Gaia data, when we will have good photometry for most background stars. The main problem lies with very red stars, which have the greatest DCR (stars, especially cool ones, are not black bodies). These are relatively rare, since they are either intrinsically very faint, or seldom short lived evolved stages. Moreover, the astrometric solution relies on more than one star, i.e. the impact will be even lower. Therefore in most cases the effect of DCR will be smaller than given in the table. Another issue is the magnitude of the target itself. Presumably (judging from our experience with other spacecraft, and considerations concerning the reflective surfaces and the illuminating source - our Sun) it will itself not be extremely red, but moderately so. In any case the colour of Gaia should, especially in the initial phase, when it is most prone to changes caused by the radiation in its harsh environment, be monitored.

Finally the all overwhelming detrimental effect on astrometric accuracy are the reference catalogues. Fortunately, this will be the one which will improve most dramatically, once Gaia data is at our disposal, after that, we can safely ignore this item(!). Before there is very little we can do to improve the situation. For this reason all old observations will be rereduced after the Gaia astrometry become available.

[16] 30'×30' FOV

Now, finally we have to assign a value to characterise the total systematic error budget (excluding precision). As shown, this is not easy and will not be very reliable. For the situation before the 1st AGIS, we will simply state that the total error comes from the reference catalogue quality and DCR. To be on the safe side, we would say 50-120 mas. After the 1st AGIS with the hitherto main source of systematic error eliminated, the situation become more complicated, since some of the items, now considered negligible, might become important. Therefore every value given here is more like an educated guess. We will try to improve on this situation with more tests, and considerations as time progresses. Right now the value would be 5-7 mas. Finally a word of caution concerning the phrase ”systematic” effect. While it is certainly true, that most of these effects influence the accuracy, they can thus be called ”systematic”, this does not imply a systematicity which is unidirectional for the whole suite of GBOT data. For any given series of measurements there will be a net systematic offset in one certain direction, but for most effects, there will not be a preferred long term direction (for the refraction there may be a residual semi-global trend in all observations from one hemisphere), therefore they will random out. Therefore the error budget subject to this paper is not to be understood as the systematic error budget, most of what is described here will contribute to the random or pseudo random error and to a lesser degrees to a global systematic error. This is to be kept in mind when perusing this report.

3.1 A reality check using existing test data

During the last years we have accumulated and reduced a significant amount of data. Therefore we can undertake a reality check. In this context we have to point at a caveat concerning the $O - C$-values used in the following part: The ”C” part, i.e. the ephemerides whose coordinates we use for comparison are of course also not error-less. Prior to spring 2012 they were not very often updated, especially not after corrective boosts, which meant, that they could be quite off. Therefore one should only look at data reduced after March 2012. It must also be noted that inaccuracies in the coordinates of the ephemerides are not part of the error budget, since they have no real connection to the complete reduction process.

The systematic error signal will mostly be in the mean offset $\overline{O - C}$, and to a lesser part in the scatter σ_{O-C}. Accordingly the scatter will also leave its trace in the mean offset, as will the inaccuracies of the ephemerides as described above. Looking at those data, the offsets are between 0 and about 120 mas, typically about 40-60 mas, usually consistent over consecutive night in absolute value or trend - this supports zonal errors in the reference catalogue being the culprit. In some cases we have trends in the offsets of one or both coordinates during one sequence - these are at current not understood, but could possibly also have their origin in reference catalogue errors, or maybe, in the loops of the ephemerides. The scatter is generally 20-60 mas in each coordinate, leading to a total r.m.s. error of 8-30 mas for a 10 exposure series. Since the movement of Planck and later Gaia during the observing time, i.e. near midnight, is much smaller than the 1°/day or 40 mas/s average we can afford to lengthen the exposure time, so that we now use 30 sec instead of 10 sec. Moreover the amount of exposures can be increased to a certain extent. Therefore we can already say now, that we are optimistic concerning meeting the precision requirement of < 20 mas. Two items need to be remarked on here: 1) because of the curved nature of the trajectory of Gaia, we will need to deliver every single datapoint (which will obviously have less precision than the whole set) and 2) all of this only holds true, if the brightness of Gaia is near where we presume it to be, i.e. near $R = 18$ mag.

4 Measures to be taken to minimise systematic effects on GBOT astrometry

The final section of this document deals with approaches to mitigate, minimise or prevent detrimental influences on the astrometric measurements. In this early version the list of measures will still be incomplete. Especially for actions which demand a certain amount of effort, we will have to consider the benefit in respect to the effort, since we want to keep the daily routine as simple and automated as possible.

It depends on the effect as described in Sect. 2, whether we can hope to avoid it through careful planning of observations, correct it, ignore it, or have to rely on mitigating damage by discarding an image or a whole sequence.

For the main factor, the reference catalogue, there is little we can do to improve the situation before the availability of Gaia data. Afterwards this factor becomes negligible. This means that - a fact which has been known to GBOT from the beginning - all data collected up to this time will have to be rereduced with Gaia astrometry being the underlying reference catalogue. While the data received after the first AGIS is most likely sufficient for GBOT purposes, we do plan to make a third pass in reducing all data of the mission at the end of the operational phase. This way we would take care that no systematic effects, which might be there after the first release of Gaia data persists[17].

Stars in the path of the target object can be located beforehand by overlaying the ephemeris on the field (as a DSS fits file and automatically checking whether and if at which time a star will be in the way. The affected institute can then be automatically warned and data taking scheduled accordingly. This feature will certainly not be installed in the beginning of operations, since other items in the pipeline development and operations setup are more pressing. It also remains to be seen whether this will be adopted by the observatories operating robotically, since they also like to keep their observing queues simple.

In many cases a stringent quality control is necessary. The exact diagnostics the pipeline supplies are still in the discussion, but one tool, which will be very useful would be a high quality high contrast zoom in on the target, so that the surroundings can be inspected. Even better

[17] Of course all systematics of the final release will be reflected in the GBOT results, the hope is that this will be very small even after the first release.

would be if a false colour palette could be used. Another effective way to get rid of single outliers in an observing sequence is to discard this one image. Care must be taken not to add extra bias; therefore only in the case one point is highly significantly deviant only this one should be discarded, if the deviation is less clear, also the most deviant point in the other direction should be omitted. This of course implies that there is an ample amount of data points, for which reason we need a standard of at least 10 data points per sequence.

Concerning the ambient conditions (sky transparency, seeing, etc.), these should be kept track by the observer/observatory, so that they are available for a posteriori inspection. Lunar phases are known anyway.

Many effects will be minimised during the astrometric reduction either by introducing an extra routine to eliminate them or by the general fitting. The Differential Refraction for example can be satisfactorily dealt with a linear term in most cases, this will be part of the general astrometric solution. For the colour refraction, we are again faced by a lack of information (about the stellar colours) in the initial phase. Therefore this can only be fully accounted for after the availability of Gaia data.

Since in principle whole sequences can be affected, it would be of great help to get feedback from ESOC on such events. The problem will just be, because of the overwhelming influence of the reference catalogue in the initial phase, most other effects will be drowned by this, therefore potential problems will only emerge after a significant amount of time has elapsed since the observations. This is unavoidable.

This section on mitigation of systematic effects will be extended in the near future, with the most important measures being listed here. Concluding we can say, that we explored as many potential sources of error as we could think of, and came to the conclusion that globally the main problem is presented by only a few of these items. We are also confident in the light of this study that we can reach and maintain a precision/accuracy of 20 mas, possibly even 10 mas.

5 Appendices

5.1 References

[MA-005], Altmann, M., Bouquillon, S., Taris, F., 2012, *Preliminary evaluation results about the suitability of the ESO VLT Survey telescope (VST) for GBOT*, `GAIA-C3-TN-ARI-MA-005`, URL `http://www.rssd.esa.int/llink/livelink/open/3128097`

Bennett, G.G., 1982, Journal of Navigation, 35, 255, ADS Link

Bertin, E., Arnouts, S., 1996, A&AS, 117, 393, ADS Link

Blau, M., 2012, *Lectures notes in General Relativity, http://www.blau.itp.unibe.ch/Lecturenotes.html*, Tech. rep., Albert Einstein Center for Fundamental Physics, Universität Bern, Switzerland

Coles, P., 2001, In: Martínez, V.J., Trimble, V., Pons-Bordería, M.J. (eds.) Historical Development of Modern Cosmology, vol. 252 of Astronomical Society of the Pacific Conference Series, 21, ADS Link

Costa, E., Méndez, R.A., Pedreros, M.H., et al., 2009, AJ, 137, 4339, ADS Link

Crosta, M.T., Mignard, F., 2006, Classical and Quantum Gravity, 23, 4853, ADS Link

Garfinkel, B., 1967, AJ, 72, 235, ADS Link

Green, R.M., 1985, *Spherical astronomy*

Gubler, J., Tytler, D., 1998, PASP, 110, 738, ADS Link

Jao, W.C., Henry, T.J., Subasavage, J.P., et al., 2005, AJ, 129, 1954, ADS Link

Méndez, R.A., Costa, E., Pedreros, M.H., et al., 2010, PASP, 122, 853, ADS Link

Monet, D.G., Dahn, C.C., Vrba, F.J., et al., 1992, AJ, 103, 638, ADS Link

Saemundsson, T., 1986, Sky&Telescope, 72, 70, ADS Link

Sinclair, A., Hohenkerk, C., 1985, *NAO Tech. Note No. 63*, Tech. rep.

Stetson, P.B., 1987, PASP, 99, 191, ADS Link

Stone, R.C., 2002, PASP, 114, 1070, ADS Link

5.2 Definitions

5.3 Acronyms

The following is a complete list of acronyms used in this document. The following table has been generated from the on-line Gaia acronym list:

Acronym	Description
AGIS	Astrometric Global Iterative Solution
AO	Announcement of Opportunity

AS	Adjacent Sample
ATP	Automatic Test Procedure
AUT	AUTomated
CCB	Configuration Control Board
CDR	Critical Design Review
CIL	Critical Items List
CM	Calibration Model
CNES	Centre National d'Etudes Spatiales (France)
CPU	Central Processing Unit
CSV	Comma-Separated Value (database output format, e.g., for MS Excel)
CU	Coordination Unit (in DPAC)
DDP	Delivered Duty Paid
DOC	Department of Commerce (USA)
DPAC	Data Processing and Analysis Consortium
DPC	Data Processing Centre
DPCE	Data Processing Centre ESAC
DU	Development Unit (in DPAC)
ECSS	European Cooperation for Space Standardisation
ESA	European Space Agency
ESAC	European Space Astronomy Centre (VilSpa)
FL	First Look
FLOP	FLoating-point OPeration
FTE	Full-Time Equivalent
GAIA	Global Astrometric Interferometer for Astrophysics (obsolete; now spelled as Gaia)
GWP	Gaia Work Package
HW	Hardware (also denoted H/W)
ICD	Interface Control Document
ID	Identifier (Identification)
IDT	Initial Data Treatment (Image Dissector Tube in Hipparcos scope)
ISO	International Organisation for Standardisation (Geneva, Switzerland)
JD	Julian Date
JDK	Java Development Kit
LaTeX	(Leslie) Lamport TeX (document markup language and document preparation system)
MAN	MANual
MDB	Main DataBase
OF	Object Feature (source packet)
PA	Product Assurance
PAP	Product Assurance Plan
PDR	Preliminary Design Review

PR	Progress Report
QA	Quality Assurance
RAM	Random Access Memory
SADT	Structured (System) Analysis and Design Technique
SCMP	Software Configuration Management Plan
SDD	Software Design Document
SDP	Supplementary Data Pattern
SP	SPecification
SPR	Software Problem Report
SRR	System Requirements Review
SRS	Software Requirements Specification
SSS	System Software Specification
STP	Software Test Plan
STR	Software Test Report
STS	Software Testing Specification
SUM	Software User Manual
SVN	SubVersioN
SW	Software
TRB	Test Review Board
TRR	Test Readiness Review
UML	Unified Modeling Language
URL	Uniform Resource Locator
WBS	Work Breakdown Structure
WP	Work Package